

Role of the Varicella-Zoster Virus gB Cytoplasmic Domain in gB Transport and Viral Egress

Thomas C. Heineman* and Susan L. Hall

*Division of Infectious Diseases and Immunology, Saint Louis University School of Medicine,
St. Louis, Missouri 63110-0250*

Received 23 August 2001/Accepted 18 October 2001

To study the function of the varicella-zoster virus (VZV) gB cytoplasmic domain during viral infection, we produced a VZV recombinant virus that expresses a truncated form of gB lacking the C-terminal 36 amino acids of its cytoplasmic domain (VZV gB-36). VZV gB-36 replicates in noncomplementing cells and grows at a rate similar to that of native VZV. However, cells infected with VZVgB-36 form extensive syncytia compared to the relatively small syncytia formed during native VZV infection. In addition, electron microscopy shows that very little virus is present on the surfaces of cells infected with VZV gB-36, while cells infected with native VZV exhibit abundant virions on the cell surface. The C-terminal 36 amino acids of the gB cytoplasmic domain have been shown in transfection-based experiments to contain both an endoplasmic reticulum-to-Golgi transport signal (the C-terminal 17 amino acids) and a consensus YXX ϕ (where Y is tyrosine, X is any amino acid, and ϕ is any bulky hydrophobic amino acid) signal sequence (YSRV) that mediates the internalization of gB from the plasma membrane. As predicted based on these data, gB-36 expressed during the infection of cultured cells is transported inefficiently to the Golgi. Despite lacking the YSRV signal sequence, gB-36 is internalized from the plasma membrane; however, in contrast to native gB, it fails to localize to the Golgi. Therefore, the C-terminal 36 amino acids of the VZV gB cytoplasmic domain are required for normal viral egress and for both the pre- and post-Golgi transport of gB.

Varicella-zoster virus (VZV) is classified as an alphaherpesvirus based on its growth characteristics and its ability to become latent in the nervous system of the host (33). Like all known herpesviruses, VZV encodes a homolog of glycoprotein B (gB) (30). While the role of gB during alphaherpesvirus entry is well established (7, 30, 31, 36), multiple lines of evidence also support the involvement of gB during herpesvirus egress. Several herpes simplex virus type 1 (HSV-1) gB mutants have been identified that induce syncytia in cultured cells (1, 4, 6). These syncytial mutations occur exclusively in the cytoplasmic domain of gB, suggesting that this region, in particular, may be critical for viral egress. Moreover, mutations in the cytoplasmic domains of both pseudorabies virus (PRV) gB and human cytomegalovirus gB alter the characteristics of cell fusion during viral infection (3, 28, 37). Also, Epstein-Barr virus gB, which is unlikely to be essential for viral entry because little, if any, is present in the virion envelope (15), is nonetheless required for the production of infectious virions, suggesting that it functions primarily during viral egress (22, 23).

Herpesvirus capsids are formed in the nucleus, and it is generally agreed that they acquire their primary envelope by budding through the inner nuclear membrane (INM) into the perinuclear space (14), which is continuous with the lumen of the endoplasmic reticulum (ER). Electron-microscopic examination of VZV-infected cells suggests that the nascent virions lose their envelopes and are released into the cytoplasm as naked capsids (13). Subsequently, they are believed to acquire their final envelope by budding into a membranous cytoplas-

mic compartment, probably the *trans*-Golgi network. In addition to the electron-microscopic data, several lines of evidence support the envelopment-deenvelopment-reenvelopment pathway for alphaherpesvirus egress: HSV-1 gD that is retained in the ER is not incorporated into virions present at the surface of cells (35); VP22, an abundant tegument protein, is found in the cytoplasm, but not the nucleus, of HSV-1-infected cells (11); and the envelopes of secreted virions have a lipid profile that differs from that of the nuclear membrane (39). Normal alphaherpesvirus egress requires several virus-encoded membrane proteins (1, 5, 24, 30, 32), and it has been hypothesized that the cytoplasmic domains of one or more viral glycoproteins mediate secondary envelopment through the interaction of their cytoplasmic domains with viral capsid or tegument proteins (14).

VZV gB is a type I membrane protein containing 868 amino acids (aa). Its cytoplasmic domain is predicted to include 125 aa, making it by far the longest cytoplasmic domain of any VZV-encoded membrane protein (11). The cytoplasmic domain of VZV gB has been shown in transfection-based experiments to contain several domains that are critical for the intracellular transport and localization of gB. First, the ER-to-Golgi transport of gB requires both the C-terminal 17 aa of its cytoplasmic domain and the region spanning aa 818 to 826 (18), and second, two consensus YXX ϕ motifs (where Y is tyrosine, X is any amino acid, and ϕ is any bulky hydrophobic amino acid), YMTL (aa 818 to 821) and YSRV (aa 857 to 860), together mediate the internalization of gB from the plasma membrane and its localization to the Golgi (17). Moreover, the importance of proper glycoprotein transport and processing during viral egress has been demonstrated experimentally. When cells defective for the intracellular transport or glyco-

* Corresponding author. Mailing address: 3635 Vista Ave., FDT-8N, St. Louis, MO 63110-0250. Phone: (314) 577-8648. Fax: (314) 771-3816. E-mail: heinemtc@slu.edu.

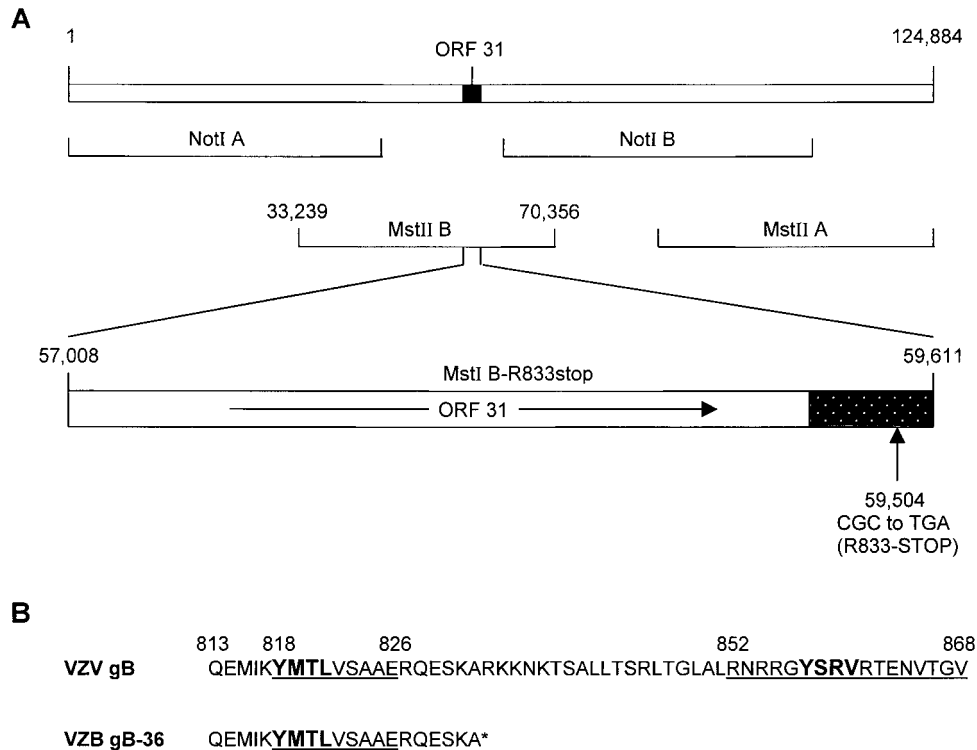


FIG. 1. Construction of recombinant VZV gB-36. (A) The prototype VZV genome (Dumas strain) is 124,884 bp in length (top line), and the position of ORF31, which encodes gB, is shown. The four overlapping cosmids used to generate infectious virus are depicted (second and third lines), and the nucleotide coordinates for the MstII B cosmid, which contains ORF31, are given. ORF31 (nucleotides 57,008 to 59,611) is expanded in the fourth line, and the direction of its translation is indicated (arrow). The shaded area represents the region of ORF31 predicted to encode the cytoplasmic domain of gB. The codon CGC at amino acid position 833 (beginning at nucleotide 59,504) within cosmid MstII B was mutated to TGA, changing it from an arginine (R) to a stop codon. (B) C-terminal amino acid sequences of native VZV gB and VZV gB-36. The numbers on top are the coordinates within gB, and the asterisk indicates the position of the stop codon that was introduced to generate the truncated form of gB. The underlined sequences were previously shown to be required for the ER-to-Golgi transport of gB, and the bold sequences are consensus YXX ϕ motifs.

sylation of viral glycoproteins are infected with HSV-1, human cytomegalovirus, or PRV, the resultant virions fail to egress normally and instead accumulate in cytoplasmic vacuoles (2, 19, 41).

To determine if the cytoplasmic domain of VZV gB is required for normal viral egress, we constructed a VZV mutant that expresses a form of gB lacking its C-terminal 36 aa (VZV gB-36) and assessed its growth properties and intracellular localization. In addition, this mutant lacks specific ER-to-Golgi and post-Golgi transport signals identified in transfection-based experiments. We therefore also assessed whether these signal sequences similarly mediate the intracellular transport of gB during VZV infection.

MATERIALS AND METHODS

Cell culture and virus propagation. MeWo cells, an immortalized human melanoma cell line, and MRC-5 cells, a diploid human fibroblast cell line, were grown in Eagle's minimum essential medium (EMEM) containing 10% fetal bovine serum (FBS; Bio-Whittaker) and GASP (2 mM L-glutamine, chlorotetracycline, penicillin, and streptomycin; Quality Biological). HFF cells, a primary fibroblast cell line derived from human foreskins, were grown in Dulbecco's modified Eagle's medium containing 10% NuSerum (Becton Dickinson) and GASP. Recombinant vaccinia virus vTF7-3 (27) was obtained from the American Type Culture Collection, and viral stocks were prepared and titered in BSC-40 cells that were grown in EMEM containing 10% FBS and GASP.

Immune reagents and intracellular markers. Anti-VZV gB monoclonal antibodies (MAbs) were purchased from Biodesign International. Goat anti-mouse immunoglobulin G conjugated with fluorescein isothiocyanate (FITC) was purchased from Sigma.

Site-directed mutagenesis. An 8,131-bp *PmeI/SpeI* fragment of VZV strain Oka (consensus nucleotides 53,876 to 62,007 [9]) containing VZV open reading frame 31 (ORF31) (the gB coding sequence; nucleotides 57,008 to 59,611), was cloned into pNEB193 (New England Biolabs) in which the *SmaI* site had been replaced with a *SpeI* linker. The 8,148-bp fragment resulting from *HindIII/SpeI* digestion of this plasmid (8,131-bp VZV DNA fragment and 17 bp from the pNEB193 polylinker) was cloned into pBluescript SK(+) (Stratagene) at the corresponding restriction sites such that the gB coding sequence was downstream of the T7 promoter to yield pBS-8131. pBS-8131 was subjected to site-directed mutagenesis with the Bio-Rad Muta-Gene phagemid in vitro mutagenesis kit, which employs the Kunkel method (21). The uracil-containing single-stranded DNA was isolated from *Escherichia coli* CJ236 after superinfection of M13KO7 helper phage (Promega). To generate VZV gB-36, the mutagenic oligonucleotide TCTAAAGCCTGAAAAAAAAT (VZV nucleotides 59,495 to 59,515; Genosys) in which VZV nucleotides 59,504 to 59,506 were changed from CGC to TGA was used. Mutagenesis of pBS-8131 with this oligonucleotide yielded pBS-8131/R833stop, in which the arginine codon at position 833 within ORF31 was replaced by a stop codon. The mutation was confirmed by sequencing the relevant region of ORF31 by the dideoxy-chain termination method (34).

Cosmid DNAs and transfections. Four cosmids containing overlapping VZV DNA fragments from the Oka strain were used for MeWo cell transfections (Fig. 1A; generously provided by Jeffrey Cohen). To produce cosmid MstI B-R833stop, pBS-8131/R833stop was cut with *PmeI* and *SpeI*, and the resulting 8,131-bp fragment was isolated. This fragment, containing the mutation

R833stop within ORF31, was then ligated into cosmid MstI B in place of the native sequences, which had been removed by digestion with *PmeI* and *SpeI*.

To produce recombinant virus, 60-mm-diameter dishes were seeded with 1.7×10^6 MeWo cells 1 day prior to transfection. Transfections were performed by the calcium phosphate method (26). Each cosmid was linearized with *NorI* or *Bsu36I*, phenol extracted, and ethanol precipitated prior to transfection. Each transfection mixture contained 0.75 μ g of cosmid MstII A, 1.5 μ g of each of the other three cosmids, 2 μ g of sheared salmon sperm DNA, and 50 ng of plasmid pCMV62 (8). Five days after transfection, the cells were seeded into 75-cm² flasks and monitored for cytopathologic effects.

Southern blots. VZV DNA was purified from nucleocapsids of infected cells, cut with *BamHI*, fractionated on a 0.8% agarose gel, and transferred to a nitrocellulose membrane. All four parental cosmid DNAs, spanning the entire VZV genome, were biotinylated with the BioNick labeling system according to the manufacturer's instructions (Gibco-BRL) and hybridized to the immobilized VZV DNA. The labeled DNA was visualized with the Photogene nucleic acid detection system (Gibco-BRL).

Growth characteristics of VZV. The VZV titers were determined by inoculating MeWo cells with serial 10-fold dilutions of virus-infected cells (16). VZV growth curves were generated by inoculating MeWo cells in 25-cm² flasks with infected cells containing approximately 100 PFU. Individual flasks were treated with trypsin, and the virus titer was determined on MeWo cells at days 1 to 6 after infection.

To compare plaque morphologies, cultured cells were inoculated with similar titers of cells infected with either native VZV or VZV containing the mutated form of gB, incubated at 37°C for 4 days, and then photographed with an inverted light microscope.

Expression of VZV gB by transfection and infection. VZV gB was expressed by in vitro transfection of pBS-8131 or pBS-8131/R833stop by the method of Fuerst et al. (12) modified as follows. DNA for transfection was column purified (Qiagen) and transfected using Lipofectin (Gibco-BRL). Cells at 75 to 90% confluence were infected with vaccinia vTF7-3 at a multiplicity of infection of 10 and then transfected with 7 μ g of DNA and 12 μ l of Lipofectin in 10-cm² wells or 3.5 μ l of DNA and 6 μ l of Lipofectin in 1.2-cm² wells. Following transfection, cells were incubated at 37°C in 5% CO₂. To express VZV gB by infection, cultured cells were inoculated with VZV-infected cells and incubated at 37°C in 5% CO₂.

Radiolabeling and immunoprecipitation of proteins. All metabolic labeling was performed at 37°C in 5% CO₂. gB expressed in vitro by transfection was labeled 16 h after transfection, and gB-infected cells were labeled when the cells exhibited extensive cytopathic effect, typically about 3 days after inoculation. For steady-state labeling, cells were incubated for 1 h in EMEM lacking cysteine and methionine (starvation period) and then incubated in Cys- and Met-free EMEM containing 125 μ Ci of Tran³⁵S-label (ICN) per ml for 4 h. To pulse-label, cells were incubated for 1 h in Cys- and Met-free EMEM containing 125 μ Ci of Tran³⁵S-label/ml without prior starvation. Following the 1-h labeling period, cells were washed and incubated for 4 h in chase medium (EMEM containing 10% FBS, 24 μ g of cysteine per ml, and 15 μ g of methionine per ml). Labeled cells were washed extensively in phosphate-buffered saline (PBS) at 4°C and lysed in PBS containing 1% Triton X-100, 0.5% deoxycholate, and 0.1% sodium dodecyl sulfate (SDS). VZV gB was immunoprecipitated by incubating the cell lysates with anti-VZV gB MAbs (1:750 dilution) overnight at 4°C followed by incubation with *Staphylococcus* protein G (Pharmacia Biotech) for 1 h at 4°C. After washing, immunoprecipitated proteins were eluted in sample buffer containing 2% SDS (Bio-Rad) and resolved by SDS-polyacrylamide gel electrophoresis (PAGE) on 8% gels. For reducing gels, 40 mM dithiothreitol was added to the sample buffer prior to elution. The gels were dried, and the labeled, immunoprecipitated proteins were visualized by autoradiography.

Carbohydrate analysis. Radiolabeled proteins were immunoprecipitated as described above and then heated at 98°C for 3 min in 10 μ l of 0.2% SDS-50 mM Tris-HCl, pH 6.8. After cooling to room temperature, 10 μ l of 0.15 M sodium citrate, pH 5.3, and 1 μ l (0.005 U) of endoglycosidase H (endo H; Boehringer Mannheim) were added. The reaction mixtures were incubated overnight at 37°C. Sample buffer was added to the endo H-treated proteins, and they were resolved by SDS-PAGE on 8% gels.

Quantitation of immunoprecipitated proteins. Following autoradiography of immunoprecipitated gB, the intensities of the endo H-resistant (high-molecular-weight [high-MW]) and endo H-sensitive (low-MW) gB signals were quantitated with a Molecular Dynamics densitometer. The proportion of endo H-resistant gB relative to total gB was determined by dividing the intensity of the endo H-resistant signal by the sum of the intensities of the endo H-resistant and endo H-sensitive signals.

Endocytosis assay. An endocytosis assay was performed, with minor modifications, as previously described (29). Briefly, MeWo cells were grown on glass

coverslips in 12-dishes (1.2 cm²/well) and infected with native VZV or VZV gB-36. Forty-eight hours after infection, the cells were incubated with anti-VZV gB MAb (1:250) for 1 h at 4°C, washed with cold PBS, and then incubated with medium containing 10% FBS at 37°C for 0 or 60 min. The cells were fixed and permeabilized in 4% paraformaldehyde containing 0.2% Triton X-100, blocked by incubation with PBS containing 1% goat serum (Sigma) for 1 h at room temperature, and then incubated for 1 h at room temperature with goat anti-mouse immunoglobulin G-FITC diluted 1:1,000 in PBS containing 1% goat serum. Following incubation with the secondary antibodies, the cells were washed in PBS and viewed with a Bio-Rad MRC 1024 laser scanning confocal microscope.

Electron microscopy. For electron microscopy, uninfected MeWo cells or MeWo cells infected with VZV were fixed in 2% glutaraldehyde in phosphate buffer (58 mM Na₂HPO₄, 18 mM KH₂PO₄, 75 mM NaCl, 2 mM CaCl₂ [pH 7.2]) overnight at 4°C. Cells were then washed twice with phosphate buffer and postfixed in 2% osmium tetroxide. Following ethanol dehydration, the cells were infiltrated with Spurr's resin, embedded in fresh Spurr's resin, and polymerized overnight at 60°C. Ultrathin sections were cut with a Leica Super Nova ultramicrotome, mounted on copper mesh grids, and stained with 2.5% uranyl acetate in 50% ethanol followed by Reynold's lead citrate. The sections were viewed and photographed with a JEOL JEM-1200EX transmission electron microscope.

RESULTS

Construction of recombinant VZV gB-36. Infectious recombinant VZV can be generated by cotransfecting four cosmid DNAs that together contain the entire VZV genome in overlapping fragments (Fig. 1A) (8). To generate a VZV recombinant that encodes gB lacking its C-terminal 36 aa (VZV gB-36), cosmid MstII B, which contains ORF31 (the gB coding sequence) (9), was mutated such that gB codon 833 was changed from CGC (arginine) to the stop codon, TGA, resulting in cosmid MstI B-R833stop (Fig. 1A). The mutated cosmid was cotransfected into MeWo cells with the remaining three native cosmid DNAs. Ten days following transfection, plaques were noted, indicating the presence of infectious virus. Two independently derived VZV gB-36 mutants were used in parallel for all experiments to minimize the possibility that an unintended mutation might have influenced the phenotype of the virus. To confirm that the resulting mutants contained the intended mutation, the region of viral DNA encoding the cytoplasmic domain of gB was amplified by PCR and sequenced. Also, Southern blot analysis of purified VZV gB-36 DNA from each mutant revealed the expected restriction fragment profiles, indicating that no large, unexpected alterations were present in the VZV gB-36 genomes (data not shown).

To demonstrate that VZV gB-36 expressed a truncated form of gB (Fig. 1B), gB was immunoprecipitated from cells infected with either native VZV or VZV gB-36 and resolved by SDS-PAGE (Fig. 2). Mature VZV gB is largely, but not entirely, posttranslationally cleaved into two disulfide-linked subunits of approximately equal sizes (20, 25). Therefore, as expected, native gB was seen both in its uncleaved 110-kDa form and as a comigrating doublet of about 60 kDa, representing its proteolytically cleaved form (Fig. 2). Uncleaved gB-36 migrated slightly faster than uncleaved native gB, consistent with the absence of its C-terminal 36 aa, which have a predicted MW of about 4,000. However, no proteolytically cleaved gB-36 is seen. These data confirm that VZV gB-36 produces a truncated form of gB. Also, as discussed below in the context of other data, the absence of the cleavage products suggests that gB-36 is transported inefficiently to the Golgi, where the posttranslational cleavage occurs.

Growth properties of VZV gB-36. To evaluate whether deletion of the C-terminal 36 aa of gB affected the growth of

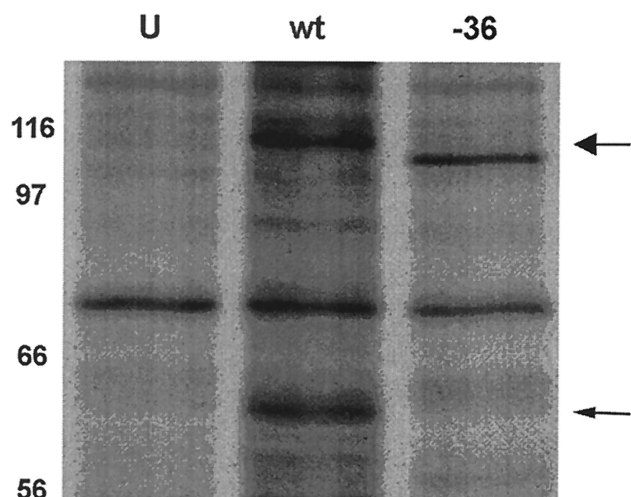


FIG. 2. Expression of gB by VZV gB-36. VZV gB was immunoprecipitated from MeWo cells infected with native VZV (wt) or VZV gB-36 (-36) and then resolved by SDS-8% PAGE under reducing conditions. Uninfected MeWo cells (U) were treated identically and served as negative controls. The high-MW uncleaved form of native gB is marked by the large arrow, and the proteolytically cleaved form of native gB, which migrates as a doublet of about 60 kDa, is indicated by the small arrow. The numbers are MW, in thousands.

VZV *in vitro*, we measured virus production by native VZV and VZV gB-36 during a 6-day growth analysis. MeWo cells were inoculated with virus-infected cells, and daily after inoculation the infected monolayers were harvested and the virus titer was determined. The yield of cells infected with VZV gB-36 was about half ($1/3 \log_{10}$) that of cells infected with native gB at day 5 (Fig. 3). This assay, however, does not measure the titer of infectious virions present within cells, which may differ between native VZV and VZV gB-36 given the highly fusogenic growth of VZV gB-36 (discussed below). Therefore, the growth analysis shown in Fig. 3 may underestimate actual virus production during VZV gB-36 infection.

While VZV gB-36 grew at a rate similar to that of native VZV, it induced far more cell fusion. To study this effect, cells were infected simultaneously with similar titers of native VZV or VZV gB-36 and examined by light microscopy 4 days later. Figure 4 shows infected MeWo cells; similar results were seen in MRC-5 and HFF cells. Native VZV-infected cells developed open plaques surrounded by rounded cells and occasional small, fused cells. In contrast, VZV gB-36-infected cells fused extensively to form giant cells containing hundreds of nuclei and formed very few small rounded cells.

Egress of VZV gB-36. The highly syncytial phenotype of cells infected with VZV gB-36 may result from a defect in viral egress. To assess this possibility, cells were infected with native VZV or VZV gB-36, and the intracellular distribution of virions was examined by electron microscopy. In both cases, nuclear capsids apparently in the process of budding into the INM were occasionally observed (Fig. 5C). Also, enveloped virions were found in the cytoplasm of cells infected with either native VZV or VZV gB-36, typically within membranous structures (Fig. 5B and C). These data indicate that neither primary envelopment at the INM nor secondary envelopment within the cytoplasm is precluded by this mutation. However, the

expression of virions on the surfaces of cells appeared to differ between native VZV and VZV gB-36 infection. As expected, native VZV particles were abundantly present on infected cell surfaces (Fig. 5A). In contrast, VZV gB-36 virions were rarely seen on the surfaces of cells, including cells that were heavily infected, as evidenced by the presence of numerous intracellular viral particles (Fig. 5B and C).

ER-to-Golgi transport of VZV gB-36. Previous transfection-based studies demonstrated that the C-terminal 17 aa of the VZV gB cytoplasmic domain are required for the ER-to-Golgi transport of gB and that gB lacking its C-terminal 36 aa (Fig. 1B) exhibited virtually no transport to the Golgi (18). To determine whether the ER-to-Golgi transport of VZV gB-36 is similarly impaired during infection, we infected cells with VZV or VZV gB-36 and evaluated the transport of gB to the Golgi by assaying for the acquisition of two distinct Golgi-dependent posttranslational modifications: proteolytic cleavage and conversion of N-linked oligosaccharides from high-mannose to complex forms.

As described earlier, gB-36 immunoprecipitated from infected cells was present only in its higher-MW, uncleaved form, in contrast to native gB, which is largely cleaved into two fragments of about 60 kDa each (Fig. 2). This indicates that during infection the C-terminal 36 aa are required for the efficient transport of gB to the Golgi, where proteolytic cleavage occurs.

In addition, VZV gB has several N-linked oligosaccharides in its ectodomain that are processed in the Golgi from their high-mannose (endo H-sensitive) to complex (endo H-resistant) forms (25). Thus, oligosaccharide maturation with the resultant acquisition of endo H resistance serves as a marker for the transport of gB from the ER to the Golgi. Figure 6

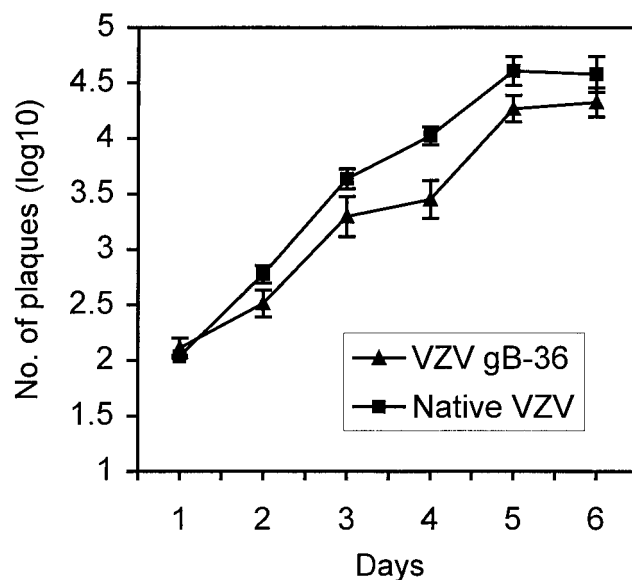


FIG. 3. Growth rate of VZV gB-36 compared to native VZV. MeWo cells were inoculated with either native VZV- or VZV gB-36-infected cells. Cells were harvested on days 1 to 6 after infection, and titers were determined on MeWo cells. The data are \log_{10} of the mean number of plaques per dish \pm standard errors of the means for three independent experiments. The day 0 value is the titer of virus in the VZV-infected-cell inocula.

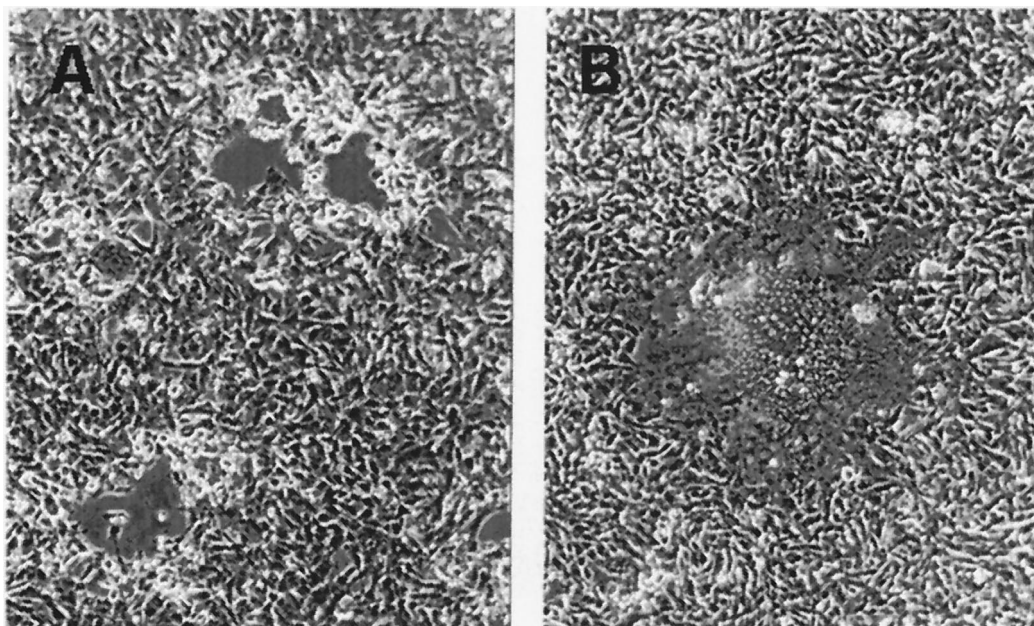


FIG. 4. Plaque morphology following infection of cells with native VZV or VZV gB-36. MeWo cell monolayers were infected with cells containing similar titers of native VZV (A) or VZV gB-36 (B) and incubated at 37°C for 4 days prior to photographing.

shows a comparison of the endo H sensitivity of native gB to that of gB-36 following both transfection and infection. MeWo cells were infected with native VZV or with VZV gB-36, or they were transfected with DNA constructs designed to express native gB or gB-36. Following either infection or transfection, the cells were pulse-labeled and incubated in chase medium for 4 h. After immunoprecipitation, gB was treated with endo H to remove high-mannose oligosaccharides. Uninfected MeWo cells were processed identically and served as negative controls. Native gB, whether expressed by transfection or infection, transited efficiently to the Golgi during the 4-h chase interval, where it acquired endo H resistance, as evidenced by the presence of the high-MW form (Fig. 6A). In contrast, VZV gB-36 expressed by transfection remained almost entirely endo H sensitive after the 4-h chase, indicating that its transport to the Golgi was markedly impaired. Similarly, the ER-to-Golgi transport of gB-36 expressed during infection was also significantly impaired, but to a lesser extent than that of gB-36 expressed by transfection (Fig. 6A).

To quantitatively compare the ER-to-Golgi transport efficiency of gB-36 expressed during infection to that of gB-36 expressed by transfection, the proportion of gB transported to the Golgi during the 4-h chase was calculated by dividing the amount of gB present as the higher-MW (endo H-resistant) species by the total amount of gB (the sum of the higher- and lower-MW species) as determined by scanning densitometry (Fig. 6B). Native gB was transported to the Golgi with similar efficiency whether expressed by infection or transfection (89 and 81%, respectively). However, gB-36 was transported to the Golgi much more efficiently during infection than transfection (31 versus 4%, respectively). This suggests that viral gene products not present during transfection may contribute to the ER-to-Golgi transport of VZV gB during infection.

Post-Golgi transport of VZV gB-36. In addition to the ER-to-Golgi transport signals, the cytoplasmic domain of VZV gB also contains two YXX ϕ motifs (Fig. 1B), both of which have been shown in transfection-based assays to participate in the post-Golgi localization of gB (17). One of these, YSRV (aa 857 to 860), is contained within the C-terminal 36 aa of VZV gB and is required for the internalization of gB from the plasma membrane in transfected cells. An internalization assay was performed to determine whether the endocytosis of gB-36 is similarly impaired during infection. Cells were infected with native VZV or VZV gB-36 and incubated with anti-gB MAbs at 4°C, resulting in the binding of these antibodies to gB present within the plasma membranes of the live cells. Internalization was then allowed to proceed at 37°C for 0 or 60 min. The cells were fixed, and after staining with FITC-conjugated secondary antibodies, the localization of gB was determined by confocal microscopy (Fig. 7). At 0 min, both native gB and gB-36 were present exclusively in the plasma membrane, as no endocytosis had yet occurred. After incubation at 37°C for 60 min, native gB was seen predominately in well-defined perinuclear structures consistent with the Golgi, as expected based on previous studies (18). However, gB-36 was dispersed diffusely throughout the cytoplasm. Therefore, despite the absence of the YSRV internalization signal, gB-36 was internalized from the plasma membrane. Following internalization, however, it failed to localize to the Golgi, suggesting that sequences within the C-terminal 36 aa are required for the normal intracellular transport of VZV gB following endocytosis.

DISCUSSION

In this study, we produced the first VZV recombinant virus that contains a mutation in gB. Our data demonstrate that the

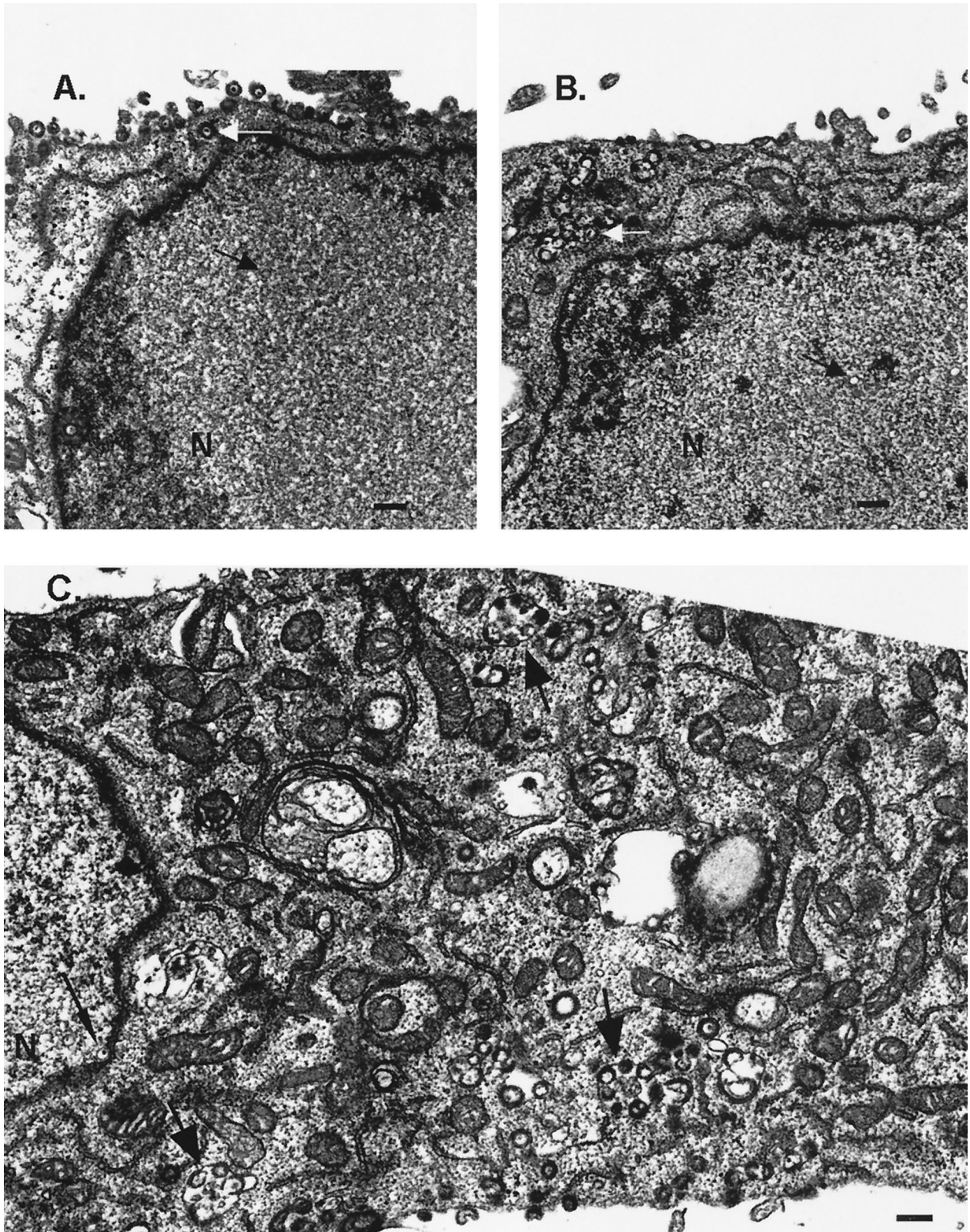


FIG. 5. Viral egress of VZV gB-36. MeWo cells were infected with native VZV (A) or VZV gB-36 (B and C). Four days after inoculation, the cells were fixed and viewed by transmission electron microscopy. (A and B) Black arrows mark intranuclear capsids, and white arrows mark intracytoplasmic virions. (C) Large arrows indicate membranous structures in the cytoplasm that contain enveloped virions, and the small arrow indicates an intranuclear capsid that appears to be budding into the INM. Bars, 250 nm.

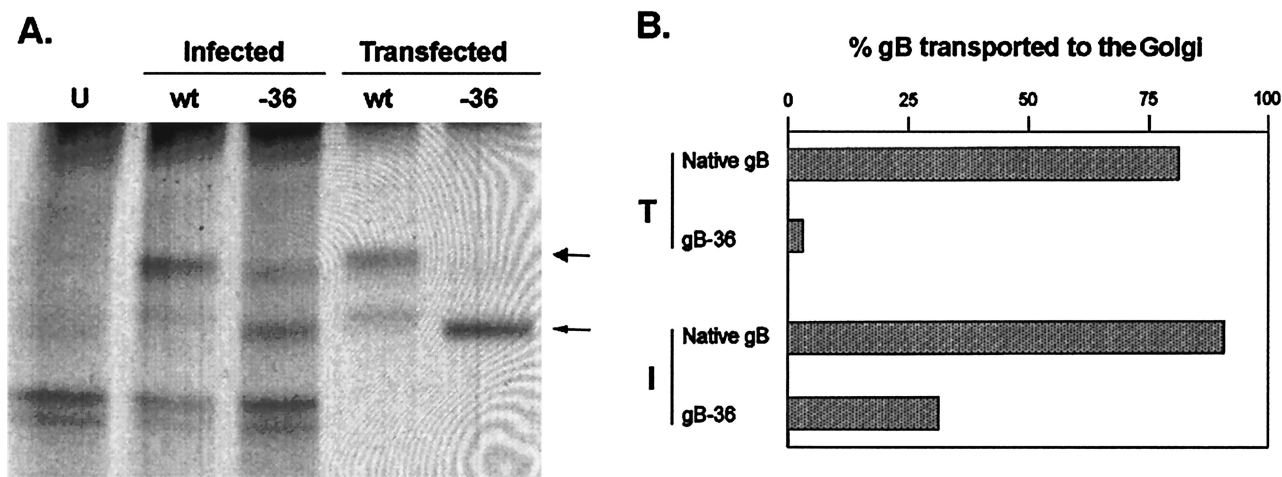


FIG. 6. ER-to-Golgi transport of gB-36. (A) MeWo cells were infected with native VZV (wt) or VZV expressing gB-36 (-36) or transfected with an expression plasmid containing the native gB or gB-36 open reading frames. VZV gB was immunoprecipitated from both the infected and transfected cells, treated with endo H, and resolved by SDS-8% PAGE under nonreducing conditions. Uninfected cells were treated identically and served as negative controls (U). The large arrow marks the high-MW endo H-resistant form of gB, and the small arrow marks the low-MW endo H-sensitive form. (B) The proportions of native gB and gB-36 expressed during transfection (T) and infection (I) were quantitated by scanning densitometry. The values are the averages of three independent experiments.

C-terminal 36 aa of VZV gB, while not essential for growth in cultured cells, are required for normal viral egress. First, VZV expressing gB-36 induces much more extensive cell fusion than native VZV infection, and second, VZV gB-36 virions, in contrast to native VZV virions, are seldom found on the surfaces of infected cells. Moreover, our data indicate that the C-terminal 36 aa of VZV gB are required for the normal transport of gB from the ER to the Golgi and that these sequences also participate in the post-Golgi localization of gB.

Significantly, the present study also demonstrates that previously described transfection-based assays (17, 18) are able to correctly identify transport signals that function during infection. Nonetheless, the transport of gB-36 during infection differed in some important respects from its transport during transfection. First, as predicted by the transfection-based studies, gB-36 expressed during infection was transported to the Golgi less efficiently than native gB. However, the ER-to-Golgi transport of gB-36 was much more efficient during infection than transfection, suggesting that one or more VZV-encoded gene products may contribute to this process. Second, in contrast to the transfection-based data, gB-36 expressed during infection was internalized from the plasma membrane despite lacking the YSRV sequence. Unlike native gB, however, gB-36 expressed during infection failed to accumulate in the Golgi. Therefore, the C-terminal 36 aa of the gB cytoplasmic domain, while not required for internalization of gB, are necessary for the correct intracellular localization of gB during infection. Our data do not precisely define the sequences within this region that are required for the Golgi localization of gB, but the YSRV sequence is perhaps the most likely candidate for this function, given its essential role in the internalization of gB following transfection (17). Furthermore, PRV lacking the C-terminal 29 aa, which contain a homologous YXX ϕ motif (YQLR), exhibits impaired internalization (28). It has been suggested that VZV gE or gI (or both) may mediate the transport of other VZV glycoproteins to the *trans*-Golgi network

(40). While recent transfection-based data demonstrate that gB can reach the Golgi without the participation of other VZV proteins (17, 18), the data presented here support the possibility that these or other VZV-encoded proteins may contribute to both the pre- and post-Golgi transport of gB during infection.

The highly syncytial phenotype of VZV gB-36 parallels the enhanced fusogenicity exhibited by comparable HSV-1 and PRV mutants lacking the C-terminal 28 and 29 aa of gB, respectively (1, 28). It has been proposed that elimination of these cytoplasmic domain sequences unmasks a fusogenic potential within gB that directly mediates cell-cell fusion, and it raises the possibility that gB may participate in the fusion of intracellular membranes during viral egress. The envelopment-deenvelopment-reenvelopment pathway, which is increasingly accepted as the route of alphaherpesvirus egress from infected cells, requires several fusion events. The first fusion event must occur as the nuclear capsid buds into the INM and acquires its primary envelope. The primary envelope must then fuse with the outer nuclear membrane (or the ER) to release naked capsids into the cytoplasm. The next membrane fusion occurs when the cytoplasmic capsid buds into a membranous structure such as the *trans*-Golgi network, resulting in a secondarily enveloped virion within an endosomal compartment. Finally, the endosome containing the mature virions must fuse with the plasma membrane to release the infectious virus. The role of gB in these individual fusion events is not known. However, VZV gB-36 virions appear to acquire both their primary and secondary envelopes, and virions can be found in cytoplasmic endosomes. Also, no abnormal-appearing collections of VZV gB-36 virus particles were observed in any intracellular compartment. Thus, viral egress, including the first three fusion events, appears to proceed in the absence of the C-terminal 36 aa of gB. However, in contrast to cells infected with native VZV, very few VZV gB-36 virions were observed on the surfaces of infected cells. This raises the possibility that the final

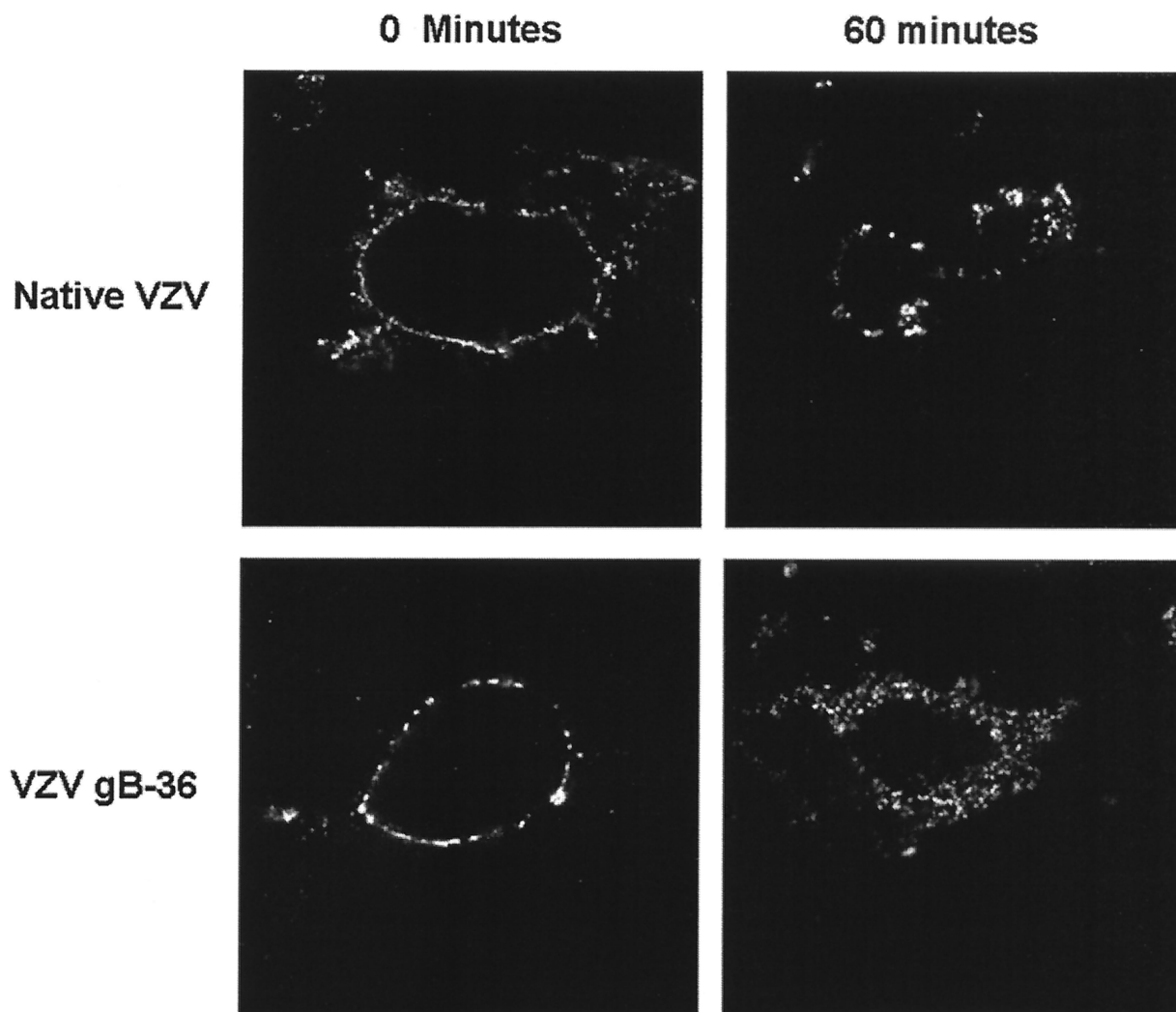


FIG. 7. Internalization of gB-36. MeWo cells were infected with native VZV or VZV gB-36, incubated with anti-VZV gB MAbs at 4°C, and placed at 37°C for 0 or 60 min. The intracellular location of gB was determined by immunofluorescent staining and confocal microscopy.

fusion event, the fusion of virus-containing endosomes with the plasma membrane, may be impaired by deletion of the C-terminal 36 aa of gB.

Alternatively, the enhanced cell fusion induced by infection with VZV gB-36 may not be directly mediated by the presence of gB-36 in the plasma membrane. Rather, it may be a by-product of impaired cell-to-cell spread of infectious VZV gB-36. As VZV is highly cell associated in culture, VZV infection propagates solely by cell-to-cell spread. During native VZV infection, syncytium formation occurs but is limited presumably by the early infection, growth disruption, and ultimate death of the adjacent cells. If infectious VZV gB-36 virions cannot spread efficiently from cell to cell, due to their inability to reach the cell surface or for some other reason, then the neighboring cells may remain uninfected and thus be available to fuse with the infected cell. Several alphaherpesvirus-encoded proteins, including gB, gH, and gM (10, 32, 38), have been shown to induce cell fusion, and these may accumulate to high levels in the plasma membrane of VZV gB-36-infected cells, resulting in enhanced cell fusion.

In addition to intracellular fusion, VZV gB may play other roles in viral egress that could be affected by eliminating the C-terminal 36 aa. It has been suggested that the cytoplasmic domains of herpesvirus glycoproteins may interact with tegument or capsid proteins during secondary envelopment within the cytoplasm (13). If the cytoplasmic domain of VZV gB functions in this capacity, then truncation of the C-terminal 36 aa may eliminate sequences essential for these interactions and thereby impair viral egress. However, as noted above, our electron micrographs showing enveloped VZV gB-36 virions in the cytoplasm of infected cells tend to argue against an essential role for the gB cytoplasmic domain during secondary envelopment. Nonetheless, it is possible that the observed intracellular virions or their envelopment in the cytoplasm are in some way abnormal due to the mutation in gB. Similarly, mutations within the cytoplasmic domain of gB may disrupt the formation of as-yet-unrecognized functional complexes between gB and other VZV proteins likely to be required for viral egress, such as the gE/gI complex (24).

Regardless of its precise function, however, the activity of

VZV gB during viral egress may depend on its localization to a specific intracellular compartment. Our data show that during infection, transport of the truncated form of gB to the Golgi is inefficient and that its post-Golgi localization is also disrupted. Therefore, the impaired egress of VZV gB-36 virions may result from the absence of gB in sufficient quantities at the intracellular location where it is required for normal viral egress.

Our data demonstrate that VZV gB is required for normal viral egress and that the C-terminal 36 aa of its cytoplasmic domain are critical not only for this process but also for the intracellular transport of gB itself. Additional studies are needed to delineate the specific function of gB during viral egress and, in particular, how its function is coordinated with that of other VZV proteins known to participate in the formation of infectious virions.

ACKNOWLEDGMENTS

We thank Nancy Galvin for her expert contributions to the electron microscopic studies and Nancy Krudwig for her valuable technical support.

This work was supported in part by NIH grant RO1 AI44905-02.

REFERENCES

1. Baghian, A., L. Huang, S. Newman, S. Jayachandra, and K. G. Kousoulas. 1993. Truncation of the carboxy-terminal 28 amino acids of glycoprotein B specified by herpes simplex virus type 1 mutant amb1511-7 causes extensive cell fusion. *J. Virol.* **67**:2396–2401.
2. Banfield, B. W., and F. Tufaro. 1990. Herpes simplex virus particles are unable to traverse the secretory pathway in the mouse L-cell mutant gro29. *J. Virol.* **64**:5716–5729.
3. Bold, S., M. Ohlin, W. Garten, and K. Radsak. 1996. Structural domains involved in human cytomegalovirus glycoprotein B-mediated cell-cell fusion. *J. Gen. Virol.* **77**:2297–2302.
4. Bond, V. C., S. Person, and S. C. Warner. 1982. The isolation and characterization of mutants of herpes simplex virus type 1 that induce cell fusion. *J. Gen. Virol.* **61**:245–254.
5. Brack, A. R., B. G. Klupp, H. Granzow, R. Tirabassi, L. W. Enquist, and T. C. Mettenleiter. 2000. Role of the cytoplasmic tail of pseudorabies virus glycoprotein E in virion formation. *J. Virol.* **74**:4004–4016.
6. Bzik, D. J., B. A. Fox, N. A. DeLuca, and S. Person. 1984. Nucleotide sequence of a region of the herpes simplex virus type 1 gB glycoprotein gene: mutations affecting rate of virus entry and cell fusion. *Virology* **13**:185–190.
7. Cai, W., B. Gu, and S. Person. 1988. Role of glycoprotein B of herpes simplex virus type 1 in viral entry and cell fusion. *J. Virol.* **62**:2596–2604.
8. Cohen, J. I., and K. E. Seidel. 1993. Generation of varicella-zoster virus (VZV) and viral mutants from four cosmids: VZV thymidylate synthetase is not essential for replication in vitro. *Proc. Natl. Acad. Sci. USA* **90**:7376–7380.
9. Davison, A. J., and J. Scott. 1986. The complete DNA sequence of varicella-zoster virus. *J. Gen. Virol.* **67**:1759–1816.
10. Davis-Poynter, N., S. Bell, T. Minson, and H. Browne. 1994. Analysis of the contributions of herpes simplex virus type 1 membrane proteins to the induction of cell-cell fusion. *J. Virol.* **68**:7586–7590.
11. Elliott, G., and P. O'Hare. 1999. Live-cell analysis of a green fluorescent protein-tagged herpes simplex virus infection. *J. Virol.* **73**:4110–4119.
12. Fuerst, T. R., E. G. Niles, F. W. Studier, and B. Moss. 1986. Eukaryotic transient-expression system based on recombinant vaccinia virus that synthesizes bacteriophage T7 RNA polymerase. *Proc. Natl. Acad. Sci. USA* **83**:8122–8126.
13. Gershon, A. A., D. L. Sherman, Z. Zhu, C. A. Gabel, R. T. Ambron, and M. D. Gershon. 1994. Intracellular transport of newly synthesized varicella-zoster virus: final envelopment in the trans-Golgi network. *J. Virol.* **68**:6372–6390.
14. Gershon, M. D., and A. A. Gershon. 1999. Role of glycoproteins in varicella-zoster virus infection, p. 43–60. *In* M. H. Wolff, S. Schunemann, and A. Schmidt (ed.), *Varicella-zoster virus molecular biology, pathogenesis and clinical aspects*. Karger, Basel, Switzerland.
15. Gong, M., and E. Kieff. 1990. Intracellular trafficking of two major Epstein-Barr virus glycoproteins, 350/220 and gp110. *J. Virol.* **64**:1507–1516.
16. Grose, C., and P. A. Brunell. 1978. Varicella-zoster virus: isolation and propagation in human melanoma cells at 36 and 32°C. *Infect. Immun.* **19**:199–203.
17. Heineman, T. C., and S. L. Hall. 2001. VZV gB endocytosis and Golgi localization are mediated by YXX ϕ motifs in its cytoplasmic domain. *Virology* **285**:42–49.
18. Heineman, T. C., N. Krudwig, and S. L. Hall. 2000. Cytoplasmic domain signal sequences that mediate transport of varicella-zoster virus gB from the endoplasmic reticulum to the Golgi. *J. Virol.* **74**:9421–9430.
19. Kari, B., R. Radeke, and R. Gehrz. 1992. Processing of human cytomegalovirus envelope glycoproteins in and egress of cytomegalovirus from human astrocytoma cells. *J. Gen. Virol.* **73**:253–260.
20. Keller, P. M., A. J. Davison, R. S. Lowe, C. D. Bennett, and R. W. Ellis. 1986. Identification and structure of the gene encoding gpII, a major glycoprotein of varicella-zoster virus. *Virology* **152**:181–191.
21. Kunkel, T. A. 1985. Rapid and efficient site-directed mutagenesis without phenotypic selection. *Proc. Natl. Acad. Sci. USA* **82**:488–492.
22. Lee, S. K., T. Compton, and R. Longnecker. 1997. Failure to complement infectivity of EBV and HSV-1 glycoprotein B (gB) deletion mutants with gBs from different human herpesvirus subfamilies. *Virology* **237**:170–181.
23. Lee, S. K., and R. Longnecker. 1998. The Epstein-Barr virus glycoprotein 110 carboxyl-terminal tail domain is essential for lytic virus replication. *J. Virol.* **71**:4092–4097.
24. Mallory, S., M. Sommer, and A. M. Arvin. 1997. Mutational analysis of the role of glycoprotein I in varicella-zoster virus replication and its effects on glycoprotein E conformation and trafficking. *J. Virol.* **71**:8279–8288.
25. Montalvo, E. A., and C. Grose. 1987. Assembly and processing of the disulfide-linked varicella-zoster virus glycoprotein gpII(140). *J. Virol.* **61**:2877–2884.
26. Moriuchi, H., M. Moriuchi, H. A. Smith, S. E. Straus, and J. I. Cohen. 1992. Varicella-zoster virus open reading frame 61 protein is functionally homologous to herpes simplex virus type I ICP0. *J. Virol.* **66**:7303–7308.
27. Moss, B., O. Elroy-Stein, T. Mizukami, W. A. Alexander, and T. R. Fuerst. 1990. Product review. New mammalian expression vectors. *Nature* **348**:91–92.
28. Nixdorf, R., B. G. Klupp, A. Karger, and T. C. Mettenleiter. 2000. Effects of truncation of the carboxy terminus of pseudorabies virus glycoprotein B on infectivity. *J. Virol.* **74**:7137–7145.
29. Olson, J. K., and C. Grose. 1997. Endocytosis and recycling of varicella-zoster virus Fc receptor glycoprotein gE: internalization mediated by a YXXL motif in the cytoplasmic tail. *J. Virol.* **71**:4042–4054.
30. Pereira, L. 1994. Function of glycoprotein B homologues of the family *Herpesviridae*. *Infect. Agents Dis.* **3**:9–28.
31. Rauh, I., and T. C. Mettenleiter. 1991. Pseudorabies virus glycoproteins gII and gp50 are essential for virus penetration. *J. Virol.* **65**:5348–5356.
32. Rodriguez, J. E., T. Moninger, and C. Grose. 1993. Entry and egress of varicella virus blocked by same anti-gH monoclonal antibody. *Virology* **196**:840–844.
33. Roizman, B. 1990. *Herpesviridae: a brief introduction*, p. 1787–1793. *In* B. N. Fields and D. M. Knipe (ed.), *Fields virology*, 2nd ed. Raven Press, New York, N.Y.
34. Sanger, R., S. Nicklen, and A. R. Coulson. 1977. DNA sequencing with chain-terminating inhibitors. *Proc. Natl. Acad. Sci. USA* **74**:5463–5467.
35. Skepper, J. N., A. Whiteley, H. Browne, and A. Minson. 2001. Herpes simplex virus nucleocapsids mature to progeny virions by an envelopment \rightarrow deenvelopment \rightarrow re-envelopment pathway. *J. Virol.* **75**:5697–5702.
36. Spear, P. G. 1993. Entry of alphaherpesviruses into cells. *Semin. Virol.* **4**:167–180.
37. Tugizov, S., Y. Wang, I. Qadri, D. Navarro, E. Maidji, and L. Pereira. 1995. Mutated forms of human cytomegalovirus glycoprotein B are impaired in inducing syncytium formation. *Virology* **209**:580–591.
38. Turner, A., B. Bruun, T. Minson, and H. Browne. 1998. Glycoproteins gB, gD, and gHgL of herpes simplex virus type 1 are necessary and sufficient to mediate membrane fusion in a Cos cell transfection system. *J. Virol.* **72**:873–875.
39. van Genderen, I. L., R. Brandimarti, M. R. Torrisi, G. Campadelli, and G. van Meer. 1994. The phospholipid composition of extracellular herpes simplex virions differs from that of host cell nuclei. *Virology* **200**:831–836.
40. Wang, Z., M. D. Gershon, O. Lungu, C. A. Panagiotidis, Z. Zhu, Y. Hao, and A. A. Gershon. 1998. Intracellular transport of varicella-zoster glycoproteins. *J. Infect. Dis.* **178**(Suppl. 1):S7–S12.
41. Whealy, M. E., J. P. Card, R. P. Meade, A. K. Robbins, and L. W. Enquist. 1991. Effect of brefeldin A on alphaherpesvirus membrane protein glycosylation and virus egress. *J. Virol.* **65**:1066–1081.